

Influence of higher-order Kerr effect on conical emission from laser filaments in gases

P. Béjot and J. Kasparian*

Université de Genève, GAP-Biophotonics, 20 rue de l'Ecole de Médecine, 1211 Geneva 4, Switzerland

**Corresponding author: jerome.kasparian@unige.ch*

We numerically investigate the conical emission (CE) from ultrashort laser filaments, both considering and disregarding the higher-order Kerr effect (HOKE). While the consideration of HOKE has almost no influence on the predicted CE from collimated beams, differences arise for tightly focused beams. This difference is attributed to the different relative contributions of the non-linear focus and of the modulational instability over the whole filament length. © 2011 Optical Society of America

OCIS codes: 320.2250, 190.2620, 190.3270, 190.5940, 190.7110, 320.7110

The filamentation of ultrashort laser pulses attracts much interest due to its spectacular potential applications [1], like remote sensing [2], lightning control [3], water condensation [4], or the generation of THz radiation [5]. Filamentation has long been described as a dynamic balance between Kerr self-focusing and defocusing by the plasma generated at the non-linear focus [1, 6–8]. However, the measurement of the saturation and inversion of the Kerr effect, described as a higher-order Kerr effect (HOKE) in air and argon [9] led us to show both numerically [10] and experimentally [11] that the HOKE can provide the main defocusing effect, especially for long wavelengths [12] and short pulses [13]. The consideration of the HOKE is also necessary to obtain a quantitative agreement of numerical models with experimental data on 3rd and 5th harmonics generation [14] and pulse propagation in hollow-core fibers [15].

However, the role of the HOKE in laser filamentation is still debated [16]. In particular, recent work [17] suggests that the experimentally observed conical emission (CE) is suppressed by the consideration of the HOKE contribution in numerical models. Conical emission [18–20] denotes the spatio-spectral distribution of the supercontinuum generated in the filaments, with a well-defined relationship between the wavelength and the emission angle. It provides an angle-resolved spectrum reflecting the complex dynamics of femtosecond pulses propagating in nonlinear dispersive media [21]. Contradictory results have been published about the

possible spectral asymmetry of CE, which is generally attributed to the temporally asymmetric distribution of the plasma along the pulse local time [7, 8, 19, 22]. However, experimental results clearly display CE on both sides of the fundamental wavelength [23]. This spectral symmetry is understood by considering either modulational instability [24, 25] or the X-wave propagation regime [21].

In this Letter, we numerically investigate the build-up of the CE along the filament length, for both collimated (parallel) and focused beams. We find that numerical models, whether considering the HOKE or not, reproduce CE on both sides of the fundamental wavelength for collimated beams, but predict qualitatively different behaviors in focused geometry. In particular, considering the HOKE is necessary to reproduce CE from focused beams, especially on the low frequency side of the spectrum.

We first simulated the propagation of a 5 mJ, 45 fs pulse (13 critical powers P_{cr}) centered at 800 nm, launched collimated in air with a radius of 3.8 mm at $1/e^2$. The code is based on the unidirectional pulse propagation equation (UPPE) [26], where we used the published values for the HOKE [9]. The model, described in detail in [11] in the case of argon, was completed by a detailed weak-field quantum modeling of the Raman-induced rotational effects in the air [27]. The far-field CE pattern is computed as Fourier (in the temporal domain) and Hankel (in the spatial domain) transforms of the electric field.

Both the full model considering the HOKE and the truncated model disregarding it predict CE on both sides of the fundamental wavelength (Figure 1). The CE angles agree perfectly with those measured experimentally in the visible [20]. In the infrared [23], the full model reproduces the CE angles slightly better, although this difference stays within the error bars.

However, the truncated model predicts a more intense conical emission than the full model. Furthermore, although both models predict the same filamentation onset distance ($z \approx 9$ m, Figure 2a), the truncated one yields a slightly earlier rise of the CE, which is more pronounced on the visible side of the spectrum (Figure 2b,c). This is especially the case at wavelengths close to the fundamental one, where the build-up of the CE appears offset by up to 1 m between the two models (See inset of Figure 2c). Comparing the outcomes of the two models in this spectral region and for this specific propagation distance [17] could therefore appear to yield a qualitative difference: The truncated model would predict significant CE while the full model would not. But the offset is short as compared with the filament length (~ 16 m), and it is difficult to practically define the filament onset in experiments and reproduce it exactly in numerical simulations [17]. Therefore, this criterion cannot in practice distinguish between the validity of the two models.

The full model predicts CE on both sides of the spectrum, regardless of the beam focusing. The latter only offsets the CE angle by an amount comparable to the numerical aperture of the focusing, and broadens the angular distribution for each spectral component (Figure

3a,c,e). Conversely, the truncated model predicts the disappearance of the CE, first on the visible side (Figure 3d), then on the infrared side (Figure 3f) of the fundamental wavelength. The resulting far-field pattern would therefore reduce to a narrow spot containing the whole continuum.

The deviations observed between the two models considering and disregarding the HOKE can be understood by considering that two processes contribute to the CE, namely the modulational instability (MI) all along the filament length, and refraction of the continuum by the refractive index gradient induced by the transverse plasma density profile. The gain of the MI contribution to CE writes [25]:

$$K = \sqrt{D(2k_0 I_0 n_{2,\text{eff}} - D) + k^{(1)2} \omega^2 I_0^2 n_{2,\text{eff}}^2} \quad (1)$$

where $D = \frac{k_\perp^2}{2k_0} - \frac{k^{(2)}\omega^2}{2}$ is the spatio-spectral dispersion operator, ω is the frequency detuning relative to the fundamental frequency, k_0 (taken at ω_0) and k_\perp the total and transverse wave vectors, $k^{(1)}$ and $k^{(2)}$ the first- and second-order dispersion term, I_0 the incident intensity and $n_{2,\text{eff}}$ the effective non-linear refractive index. For $n_{2,\text{eff}} < 0$, the gain cancels and the supercontinuum emission is confined on the beam axis [25]. Conversely, since the electron density accumulates over the pulse duration, its contribution intrinsically bears a strong temporal asymmetry, which converts into a spectral one, because dispersion and self-phase modulation red-shift the front of the pulse and blue-shift its trail. Furthermore, the plasma contribution can be considered as negligible in the framework of the full model, where the plasma density is insufficient to significantly influence the pulse propagation.

Compared to the full model, the truncated one predicts a nonlinear refractive index inversion at a higher intensity [10], resulting in a higher MI gain, hence in an earlier growth of CE at the filament onset, followed by a larger intensity. Furthermore, the high-intensity peak predicted at $z \approx 9$ m by the truncated model (Figure 2a) will result in high plasma density at the filament onset, offering a supplementary boost to the early CE emission on the visible side of the spectrum.

Tighter focusing results in higher plasma densities, especially in the framework of the truncated model. This plasma density accumulating during the pulse results in an increasingly negative contribution to $n_{2,\text{eff}}$, ultimately inverting it to negative values preventing CE. Focusing tighter will yield to an earlier inversion of $n_{2,\text{eff}}$, extinguish CE from MI first on the visible side of the fundamental, and then on the infrared side, as displayed in Figure 3d,f.

In conclusion, we have investigated the dynamics of the build-up of CE along the filamentation of ultrashort laser pulses. CE is emitted from the whole filament length through MI [25]. For collimated beams, which yield long filaments, the contribution of the non-linear focus region is moderate. Consequently, the consideration of the HOKE has no practical impact on the predicted CE. For tightly focused beams, the high plasma density predicted if the

HOKE are disregarded would lead to expect the extinction of CE. Our work therefore sheds a new light on the physics of CE, and on the need to consider its emission from the whole filament length. It also suggests the behavior of CE at tight focusing as an experimental test of the need to consider the HOKE to adequately describe CE from laser filaments.

Acknowledgements. This work was supported by the Swiss NSF (contract 200021-125315).

References

1. J. Kasparian and J.-P. Wolf. *Physics and applications of atmospheric nonlinear optics and filamentation*. Opt. Express **16**, 466 (2008).
2. J. Kasparian, M. Rodriguez, G. Mejean, J. Yu, E. Salmon, H. Wille, R. Bourayou, S. Frey, Y. B. André, A. Mysyrowicz, R. Sauerbrey, J. P. Wolf, and L. Woste. *White-light filaments for atmospheric analysis*. Science **301**, 61-64, (2003).
3. J. Kasparian, R. Ackermann, Y.-B. André, G. Méchain, G. Méjean, B. Prade, P. Rohwetter, E. Salmon, K. Stelmaszczyk, J. Yu, A. Mysyrowicz, R. Sauerbrey, L. Wöste, and J.-P. Wolf, *Electric Events Synchronized with Laser Filaments in Thunderclouds*. Opt. Express. **16**, 5757 (2008)
4. P. Rohwetter, J. Kasparian, K. Stelmaszczyk, S. Henin, N. Lascoux, W. M. Nakaema, Y. Petit, M. QueiBer, R. Salamé, E. Salmon, Z.Q. Hao, L. Wöste, J.-P. Wolf, *Laser-induced water condensation in air*. Nature Photon., **4**, 451 (2010)
5. S. Tzortzakis, G. Méchain, G. Pantalano, Y. B. André, B. Prade, M. Franco, A. Mysyrowicz, J. M. Munier, M. Gheudin, G. Beaudin, and P. Encrenaz, *Coherent subterahertz radiation from femtosecond infrared filaments in air*. Opt. Lett., **27**, 1944 (2002)
6. S. L. Chin, S. A. Hosseini, W. Liu, Q. Luo, F. Theberge, N. Aközbek, A. Becker, V. P. Kandidov, O. G. Kosareva, and H. Schroeder. *The propagation of powerful femtosecond laser pulses in optical media: physics, applications, and new challenges* Can. J. Phys. **83**, 863 (2005).
7. L. Bergé, S. Skupin, R. Nuter, J. Kasparian, and J.-P. Wolf. *Ultrashort filaments of light in weakly-ionized, optically-transparent media* Rep. Prog. Phys. **70**, 1633 (2007).
8. A. Couairon and A. Mysyrowicz. *Femtosecond filamentation in transparent media* Phys. Rep., **441** 47 (2007).
9. V. Loriot, E. Hertz, O. Faucher, B. Lavorel, *Measurement of high-order Kerr refractive index of major air components*. Opt. Express **16**, 13429 (2009); Erratum in Opt. Express **18** 3011 (2010)
10. P. Béjot, J. Kasparian, S. Henin, V. Loriot, T. Vieillard, E. Hertz, O. Faucher, B. Lavorel, and J.-P. Wolf, *Higher-order Kerr terms allowing ionization-free filamentation in air*. Phys. Rev. Lett. **104**, 103903 (2010)
11. P. Béjot, E. Hertz, J. Kasparian, B. Lavorel, J.-P. Wolf, O. Faucher, *Transition*

- from plasma- to Kerr-driven laser filamentation* Phys. Rev. Lett., to be published. arXiv:1103.1467, 9 March 2011
12. W. Ettoumi, P. B ejot, Y. Petit, V. Loriot, E. Hertz, O. Faucher, B. Lavorel, J. Kasparian, J.-P. Wolf *Spectral dependence of all-Kerr driven filamentation in air and argon*, Phys. Rev. A **82**, 033826 (2010)
 13. V. Loriot, P. B ejot, W. Ettoumi, Y. Petit, J. Kasparian, S. Henin, E. Herz, B. Lavorel, O. Faucher, and J.-P. Wolf. *On negative higher-order Kerr effect and filamentation*, Laser Physics, in press, DOI: 10.1134/S1054660X11130196
 14. P. B ejot, E. Hertz, B. Lavorel, J. Kasparian, J.-P. Wolf, O. Faucher, *From higher-order Kerr nonlinearities to quantitative modeling of third and fifth harmonic generation in argon*. Optics Letters, **36**, 828-830 (2011)
 15. P. B ejot, B. E. Schmidt, J. Kasparian, J.-P. Wolf, F. Legar e, *IR pulse compression with bulk material: comparing experiments and simulations*. Phys. Rev. A **81**, 063828 (2010)
 16. P. Polynkin, M. Kolesik, E. M. Wright, and J. V. Moloney, *Experimental Tests of the New Paradigm for Laser Filamentation in Gases*, Phys. Rev. Lett. **106**, 153902 (2011)
 17. O. Kosareva, J.-F. Daigle, N. Panov, T. Wang, S. Hosseini, S. Yuan, G. Roy, V. Makarov, S. L. Chin, *Arrest of self-focusing collapse in femtosecond air filaments: higher-order Kerr or plasma defocusing?* Optics Letters, **36**, 1035 (2011)
 18. E.T.J. Nibbering, P.F. Curley, G. Grillon, B.S. Prade, M.A. Franco, F. Salin, and A. Mysyrowicz, *Conical emission from self-guided femtosecond pulses in air*. Opt. Lett.. **21**, 62 (1996)
 19. O.G. Kosareva, V.P. Kandidov, A. Brodeur, C.Y. Chen, and S.L. Chin, *Conical emission from laser-plasma interactions in the filamentation of powerful ultrashort laser pulses in air*. Opt. Lett. **22**, 1332(1997)
 20. P. Maioli, R. Salam e, N. Lascoux, E. Salmon, P. B ejot, J. Kasparian, and J.-P. Wolf, *Ultraviolet-visible conical emission by multiple laser filaments*. Opt. Express. **17**, 4726 (2009)
 21. D. Faccio, P. Di Trapani, S. Minardi, A. Bramati, F. Bragheri, C. Liberale, V. Degiorgio, A. Dubietis, and A. Matijosius, *Far-field spectral characterization of conical emission and filamentation in Kerr media*. J. Opt. Soc. Am. B, **22**,. 862 (2005)
 22. D. Faccio, A. Averchi, A. Lotti, P. Di Trapani, A. Couairon, D. Papazoglou, S. Tzortzakis, *Ultrashort laser pulse filamentation from spontaneous XWave formation in air*. Opt. Express **16**, 1565 (2008)
 23. F. Th eberge, M. Ch ateau-neuf, V. Ross, P. Mathieu, and J. Dubois, *Ultrabroadband conical emission generated from the ultraviolet up to the far-infrared during the optical filamentation in air*. Opt. Lett. **33**, 2515-2517 (2008)
 24. G. G. Luther, A. C. Newell, J. V. Moloney, and E. M. Wright *Short-pulse conical emission*

- and spectral broadening in normally dispersive media.* Optics letters, **19**, 789 (1994)
25. P. B ejot, B. Kibler, E. Hertz, B. Lavorel, O. Faucher *General approach to spatiotemporal modulational instability processes.* Phys. Rev. A **83**, 013830 (2011)
 26. M. Kolesik, J. V. Moloney and M. Mlejnek, *Unidirectional Optical Pulse Propagation Equation.* Phys. Rev. Lett. **89**, 283902 (2002).
 27. R. A. Bartels, T. C. Weinacht, S. R. Leone, H. C. Kapteyn, and M. M. Murnane *Phase Modulation of Ultrashort Light Pulses using Molecular Rotational Wave Packets* Phys. Rev. Lett. **88**, 013903 (2002)

List of Figures

- 1 (Color online) Far-field angularly-resolved spectrum of 5 mJ, 45 fs pulses centered at 800 nm, after 24 m of propagation in air, including 16 m of filamentation. (a) Full model considering the HOKE; (b) Truncated model disregarding the HOKE. White dots display the experimental data of Théberge et al. [23] and Maioli et al. [20] on the IR and visible sides of the spectrum, respectively. 8
- 2 (Color online) Build-up of the conical emission from a 5 mJ, 45 fs pulse centered at 800 nm. (a) Total on-axis intensity; (b-d) Intensity of the CE lobe at (b) 500 nm; (c) 700 nm and (d) 1500 nm as a function of propagation distance, as predicted by the full model considering the HOKE and the truncated model disregarding the HOKE. Note that panels b-d share a common intensity scale. 9
- 3 (Color online) Far-field angularly-resolved spectrum of 1 mJ, 30 fs pulses ($4 P_{cr}$) centered at 800 nm, with a radius of 3 mm at $1/e^2$. (a,b) $f = 4$ m, $f/\# = 1333$; (c,d) $f = 2$ m, $f/\# = 667$; (e,f) $f = 1$ m, $f/\# = 333$, in the case of the full model considering the HOKE (a,c,e) and of the truncated model disregarding the HOKE (b,d,f) 10

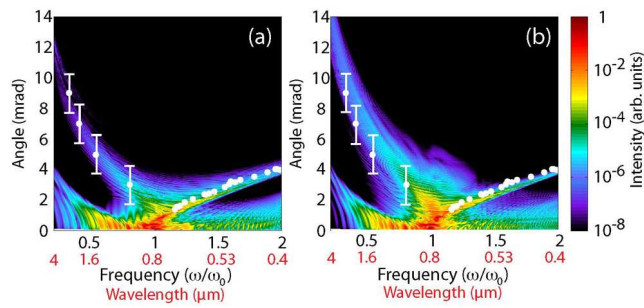


Fig. 1. (Color online) Far-field angularly-resolved spectrum of 5 mJ, 45 fs pulses centered at 800 nm, after 24 m of propagation in air, including 16 m of filamentation. (a) Full model considering the HOKE; (b) Truncated model disregarding the HOKE. White dots display the experimental data of Théberge et al. [23] and Maioli et al. [20] on the IR and visible sides of the spectrum, respectively.

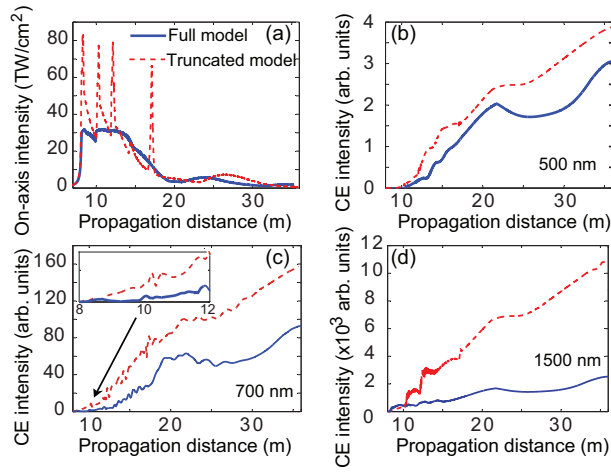


Fig. 2. (Color online) Build-up of the conical emission from a 5 mJ, 45 fs pulse centered at 800 nm. (a) Total on-axis intensity; (b-d) Intensity of the CE lobe at (b) 500 nm; (c) 700 nm and (d) 1500 nm as a function of propagation distance, as predicted by the full model considering the HOKE and the truncated model disregarding the HOKE. Note that panels b-d share a common intensity scale.

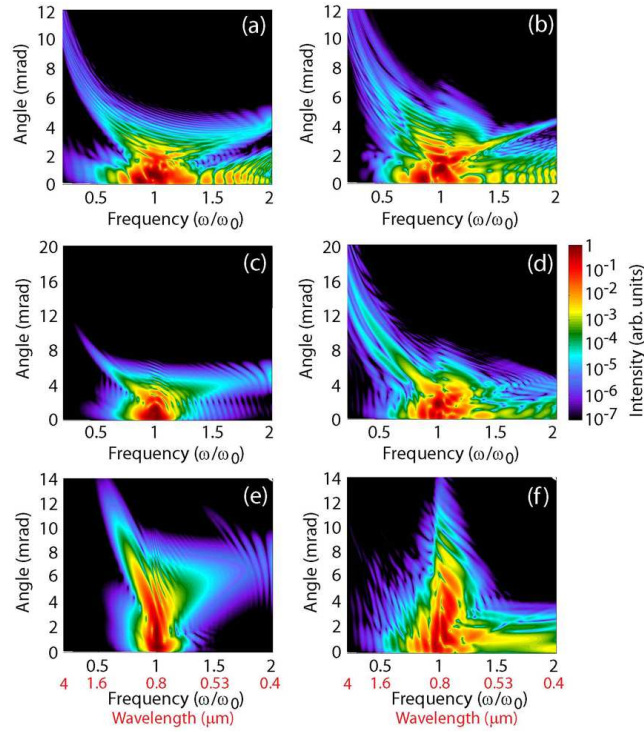


Fig. 3. (Color online) Far-field angularly-resolved spectrum of 1 mJ, 30 fs pulses ($4 P_{cr}$) centered at 800 nm, with a radius of 3 mm at $1/e^2$. (a,b) $f = 4$ m, $f/\# = 1333$; (c,d) $f = 2$ m, $f/\# = 667$; (e,f) $f = 1$ m, $f/\# = 333$, in the case of the full model considering the HOKE (a,c,e) and of the truncated model disregarding the HOKE (b,d,f)